Письма в ЭЧАЯ. А. 2011. Т. 8, № 8. С. 117–124

RECENT APPLICATIONS OF THERMUS

S. Wheaton [a,1], *M. Hauer* [b]

[a] UCT-CERN Research Centre and Department of Physics,
University of Cape Town, Cape Town, South Africa

[b] Helmholtz Research School, University of Frankfurt, Frankfurt, Germany

Some of the most recent applications of the statistical-thermal model package, THERMUS, are reviewed. These applications focus on fluctuation and correlation observables in an ideal particle and antiparticle gas in limited momentum space segments, as well as in a hadron resonance gas. In the case of the latter, a Monte Carlo event generator, utilizing THERMUS functionality and assuming thermal production of hadrons, is discussed. The system under consideration is sampled grand canonically in the Boltzmann approximation. A reweighting scheme is then introduced to account for conservation of charges (baryon number, strangeness, electric charge) and energy and momentum, effectively allowing for extrapolation of grand canonical results to the microcanonical limit. The approach utilized in this and other applications suggests improvements to existing THERMUS calculations.

PACS: 24.10.Pa

INTRODUCTION

The statistical hadronization model, first introduced by Fermi [1] and Hagedorn [2], has been remarkably successful in the description of experimentally measured average hadron production yields in heavy-ion collisions ranging from SIS [3], and AGS [4], over SPS [5] to RHIC [6] energies. Over time, this has led to the establishment of the «chemical freeze-out line» [7], which is now a vital part of our understanding of the phase diagram of strongly interacting matter. In fact, model predictions for the upcoming LHC and future FAIR [8, 9] experiments largely follow these trends. Early applications of the statistical-thermal model package, THERMUS [10], to hadron multiplicities and other average properties of the fireball have, indeed, contributed to this knowledge and understanding.

Somewhere above the freeze-out line in the phase diagram we expect, in general, a phase transition from hadronic degrees of freedom to a phase of deconfined quarks and gluons, generally termed the quark gluon plasma; and more specifically, a first order phase transition at low temperature and high baryon chemical potential, and a cross-over at high temperature and low baryon chemical potential. In between, a second order endpoint or a critical point might emerge (for recent reviews, see [11, 12]).

Fluctuation and correlation observables are amongst the most promising candidates for signaling the formation of new states of matter, such as the quark gluon plasma, and transitions between them (for recent reviews here, see [13–16]). The statistical properties of a sample

[1] E-mail: spencer.wheaton@uct.ac.za

of events are, however, certainly not solely determined by critical phenomena. More broadly speaking, they depend strongly on the way events are chosen for the analysis, and on the information available about the system.

In order to discern interesting behavior of fluctuation and correlation observables from the ordinary, a full understanding of these quantities is required within a simple and intuitive model. Given the success of the ideal gas approximation of the statistical-thermal model in describing experimentally measured average hadron yields, and its ability to reproduce low temperature lattice susceptibilities [17], the question arises as to whether fluctuation and correlation observables also follow the trends it suggests. This was the motivation for the recent effort invested in applying THERMUS in these areas.

The first system considered for fluctuation and correlation calculations using THERMUS tools was that of an ideal particle and antiparticle gas [18], while this analysis was extended to a hadron resonance gas in [19]. The underlying approach was developed and discussed in a series of papers including [20–22].

In this paper, the particular approach adopted to evaluate correlation and fluctuation observables within various ensembles of the statistical-thermal model is introduced in Sec. 1. Results from the particle and antiparticle gas study are discussed in Sec. 2, while the hadron resonance gas analysis is described in Sec. 3. The paper concludes with a discussion of topics for further development of THERMUS.

1. FLUCTUATION AND CORRELATION CALCULATIONS: FORMALISM AND NOTATION

The standard approach in statistical mechanics is to start with a MicroCanonical Ensemble (MCE), in which the energy and momentum, as well as the charge contents of a system are exactly conserved, and then introduce an infinite thermal bath with which the system of interest is able to exchange energy and momentum. A thermal parameter, the temperature, is introduced to set the average energy content of the system, thereby constituting the Canonical Ensemble (CE). Allowing the system to exchange particles (and hence charges) with the bath leads to the introduction of chemical potentials for each conserved quantum number (to set average quantum contents) and the so-called Grand Canonical Ensemble (GCE) is born.

In the approach fully discussed in [20], the grand canonical ensemble is the starting point, and the canonical and microcanonical partition functions are obtained, up to a multiplicative factor, through projection of the grand canonical partition function. The result is a canonical and microcanonical partition function expressed as integrals over functions depending on chemical potentials and temperature. As shown explicitly in [18], when analytic integration is possible, the result for the partition functions is independent of the temperature and chemical potentials. When numerical integration is performed, the choice of these parameters affects only the quality of the approximation, with the integrand oscillation-free and easily integrable in the large volume limit when the thermal parameters are chosen to correspond with those of the associated grand canonical ensemble.

As an example, the microcanonical partition function $Z_{\mathrm{MCE}}^{\mathbf{Q},\mathbf{P}}$ corresponding to a conserved charge vector $\mathbf{Q} = (B, S, Q, \ldots)$ and energy-momentum four-vector P^{μ}, is related to the

«projected-out» grand canonical partition function $\mathcal{Z}^{\mathbf{Q},\mathbf{P}}$ in the following way:

$$\mathcal{Z}^{\mathbf{Q},\mathbf{P}}\left(V,\beta,\boldsymbol{\mu},\mathbf{u}\right) \equiv \int_{-\pi}^{+\pi} \frac{d^J\phi}{\left(2\pi\right)^J} \mathrm{e}^{-iQ^j\phi_j} \int_{-\infty}^{+\infty} \frac{d^4\alpha}{\left(2\pi\right)^4} \mathrm{e}^{-iP^\mu\alpha_\mu} \times$$

$$\times \exp\left[V\sum_l \psi_l\left(\beta,\beta\boldsymbol{\mu}\rightarrow\beta\boldsymbol{\mu}+i\boldsymbol{\phi},\beta\mathbf{u}\rightarrow\beta\mathbf{u}-i\boldsymbol{\alpha}\right)\right], \tag{1}$$

$$= \mathrm{e}^{\beta Q^j\mu_j}\, \mathrm{e}^{-\beta P^\mu u_\mu} Z^{\mathbf{Q},\mathbf{P}}_{\mathrm{MCE}}\left(V,\mathbf{u}\right), \tag{2}$$

where the summation runs over all hadrons included in the gas, the single-particle partition functions ψ_l are given by their usual expressions, $\boldsymbol{\mu} = (\mu_B, \mu_S, \mu_Q, \ldots)$ is the vector of chemical potentials and, $\boldsymbol{\phi} = (\phi_B, \phi_S, \phi_Q, \ldots)$ is the vector of corresponding projection angles, while the vector of angles $\boldsymbol{\alpha}$ enforces the energy-momentum conservation. The system is assumed to have volume V, inverse temperature β, and four-velocity u_μ.

Now, probabilities within any ensemble can be expressed as the ratio of the number of states satisfying the condition of interest to the partition function of the ensemble. Furthermore, probabilities within the canonical and microcanonical ensemble can be expressed as conditional grand canonical probabilities. As an example, assuming only one conserved charge, Q, the probability within the Q-canonical ensemble of having N_A particles of type A and N_B particles of type B is given by

$$P_{\mathrm{CE}}\left(N_A,N_B\right) = \frac{Z^{Q,N_A,N_B}_{\mathrm{CE}}}{Z^{Q}_{\mathrm{CE}}}, \tag{3}$$

$$= P_{\mathrm{GCE}}\left(Q,N_A,N_B\right) P^{-1}_{\mathrm{GCE}}\left(Q\right), \tag{4}$$

$$= P_{\mathrm{GCE}}\left(N_A,N_B|Q\right), \tag{5}$$

where $P_{\mathrm{GCE}}\left(N_A,N_B|Q\right)$ is the grand canonical conditional distribution of multiplicities N_A and N_B at fixed charge Q. As is further shown in [20], grand canonical ensemble joint distributions of extensive quantities converge to multivariate normal distributions in the thermodynamic limit. In this way approximations to multiplicity distributions in canonical and microcanonical ensembles are easily found.

Once multiplicity distributions are known, fluctuations and correlations can be quantified through calculation of the scaled variance ω_i and correlation coefficient ρ_{ij}, defined as

$$\omega_i \equiv \frac{\langle\left(\Delta X_i\right)^2\rangle}{\langle X_i\rangle} \quad \text{and} \quad \rho_{ij} \equiv \frac{\langle\Delta X_i \Delta X_j\rangle}{\sqrt{\langle\left(\Delta X_i\right)^2\rangle\langle\left(\Delta X_j\right)^2\rangle}}. \tag{6}$$

2. PARTICLE–ANTIPARTICLE GAS

In [18], fluctuation and correlation observables are investigated in limited momentum space bins in a pion gas within the microcanonical ensemble in the large volume approximation. Some representative results are shown in Fig. 1. Clearly visible is the suppression, relative

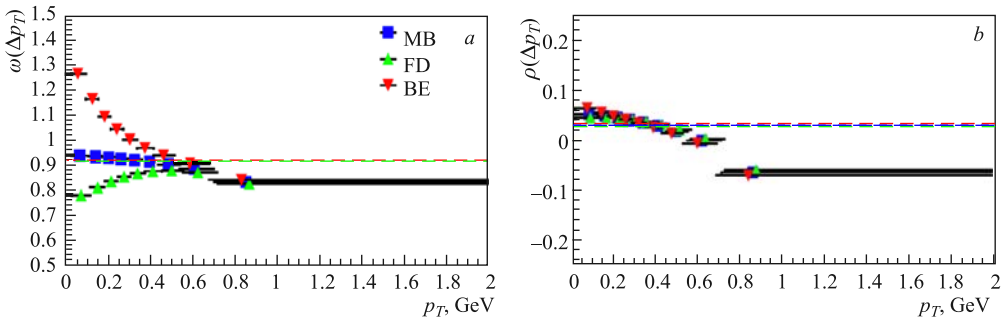

Fig. 1. Transverse momentum dependence of the MCE scaled variance of negatively charged particles (a) and the MCE correlation coefficient between positively and negatively charged particles at $T = 160$ MeV for a Boltzmann, Fermi–Dirac, and Bose–Einstein «pion gas» at zero charge density. Momentum bins are constructed such that each bin contains the same fraction q of the average π^- yield. The horizontal bars indicate the width of the Δp_T bins, while the marker indicates the position of the center of gravity of the corresponding bin. Dashed lines indicate acceptance scaling results

to Boltzmann statistics, of fluctuations at low p_T in the case of Fermi–Dirac statistics and their enhancement for Bose–Einstein statistics. While positive and negative particles are positively correlated in low-momentum bins (as expected due to charge conservation), in high-momentum bins they may even be anticorrelated (see Fig. 1, b).

Also shown in this work is the presence of long-range correlations between any two distinct regions of momentum space, even in the absence of any dynamical effects. While energy conservation leads to anticorrelation between different momentum space bins, charge correlation leads to a positive correlation of unlike charged particles. Longitudinal momentum conservation was also shown to have a large effect on correlations between distinct momentum regions, leading to interesting structure [18].

3. HADRON RESONANCE GAS

Having investigated the pion gas in some detail, attention then turned to the hadron resonance gas employed in THERMUS V2.1 (all hadrons with u, d, and s quarks up to a mass of 2.6 GeV). To introduce the scheme that was adopted, a microcanonical ensemble system of volume V_g is conceptually divided into two subsystems of volume V_1 and V_2. These subsystems are assumed to be in equilibrium with each other, and subject to the constraints of joint energy-momentum and charge conservation. Particles are only measured in one subsystem (V_1), while the second subsystem (V_2) provides a thermodynamic bath. By keeping the size of the first subsystem fixed, while varying the size of the second, one can thus study the dependence of statistical properties of an ensemble on the fraction of the system observed (i.e., assess their sensitivity to globally applied conservation laws). The starting point of the work done in [19] is a grand canonical ensemble sample $P_{\mathrm{GCE}}(P_1^\mu, Q_1^j, N_1^i|\beta, u_\mu, \mu_j)$ of Monte Carlo events of a system of temperature β^{-1}, collective velocity u^μ, and chemical potentials μ^j. Based on the values of corresponding extensive quantities, four-momentum P_1^μ and charges Q_1^j of each event, a weight factor $\mathcal{W}$ is calculated, accounting for the finite size of the bath. The vector $Q_1^j = (B_1, S_1, Q_1)$ summarizes the baryon number, strangeness,

and electric charge of the observed system, while N_1^i denotes the particle multiplicities of all particle species i considered in the model. We therefore obtain a contracted distribution:

$$P_\lambda(P_1^\mu, Q_1^j, N_1^i) = \mathcal{W}^{P_1^\mu, Q_1^j; P_g^\mu, Q_g^j}(V_1; V_g|\beta, u_\mu, \mu_j) P_{\rm GCE}(P_1^\mu, Q_1^j, N_1^i|\beta, u_\mu, \mu_j). \quad (7)$$

Provided the combined system is sufficiently large, the system in V_1 will hence carry on average a certain fraction $\lambda \equiv V_1/V_g$ of the total charge $\langle Q_1^j \rangle = \lambda Q_g^j$ and four-momentum $\langle P_1^\mu \rangle = \lambda P_g^\mu$. Statistical moments of the distributions can be calculated as

$$\langle X_i^n X_j^m \rangle = \sum_{X_i, X_j} X_i^n X_j^m P(X_i, X_j) \ , \quad (8)$$

with the variance $\langle (\Delta X_i)^2 \rangle = \langle X_i^2 \rangle - \langle X_i \rangle^2$ and covariance $\langle \Delta X_i \Delta X_j \rangle = \langle X_i X_j \rangle - \langle X_i \rangle \langle X_j \rangle$ of particular importance.

The weight factor $\mathcal{W}^{P_1^\mu, Q_1^j; P_g^\mu, Q_g^j}(V_1; V_g|\beta, u_\mu, \mu_j)$ generates an ensemble with statistical properties different from the limiting cases $V_g \to V_1$ (MCE), and $V_g \to \infty$ (GCE), allowing for extrapolation of GCE results to the MCE limit.

As an illustration of the results, we present here the microcanonical multiplicity fluctuations and correlations. Multiplicity fluctuations and correlations are qualitatively affected by the choice of ensemble and are directly sensitive to the fraction of the system observed. For vanishing size of an acceptance window, one would lose all information on how the multiplicities of any two distinct groups N_i and N_j of particles are correlated, and measure $\rho_{ij} = 0$.

In Fig. 2 we show the $\Delta p_{T,i}$ dependence of the scaled variance ω_+ (plot a), and correlation coefficient ρ_{+-} (plot b), both primordial and final state, in the MCE. Momentum bins $\Delta p_{T,i}$ are constructed such that each bin holds one fifth of the total average particle yield. The average baryon number, strangeness, and electric charge in each bin is equal to zero, as the system is assumed to be neutral. In the primordial GCE Boltzmann case one finds no dependence of multiplicity fluctuations and correlations on the position and size of the

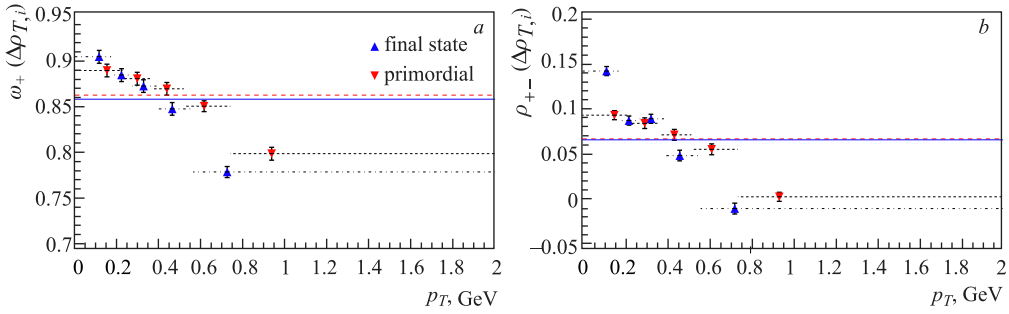

Fig. 2. MCE scaled variance ω_+ of positively charged hadrons (a), and correlation coefficient ρ_{+-} (b) between positively and negatively charged hadrons, both primordial and final state, in transverse momentum bins $\Delta p_{T,i}$. Vertical error bars indicate the statistical uncertainty of $8 \cdot 20$ Monte Carlo runs of $2 \cdot 10^5$ events each. The solid and the dashed lines show final state and primordial acceptance scaling estimates, respectively

acceptance window. The observed multiplicity distribution is the product of two Poissonians with $\omega_+ = 1$ and $\rho_{+-} = 0$. Resonance decay is the only source of correlation in the GCE.

In the MCE the situation is qualitatively different. A change in particle number at high p_T involves a large amount of energy. In order to balance the energy record, one needs to create (or annihilate) either a lighter particle with more kinetic energy, or two particles at lower p_T. By the same argument, it seems favorable to balance electric charge, by creating (or annihilating) pairs of oppositely charged particles, predominantly in lower $\Delta p_{T,i}$ bins, while allowing for a more uncorrelated multiplicity distribution, i.e., also larger net-charge ($\delta Q = N_+ - N_-$) fluctuations, in higher $\Delta p_{T,i}$ bins.

Resonance decay and conservation laws work in the same direction, as far as the transverse momentum dependence of ω_+ and ρ_{+-} is concerned. Both effects lead to increased multiplicity fluctuations and an increased correlation between the multiplicities of oppositely charged particles in the low-p_T region, compared to the high-p_T domain.

SUMMARY

In summary, THERMUS has been successfully applied to fluctuation and correlation studies within the statistical-thermal model. Furthermore, this work has highlighted several areas in which THERMUS calculations can be improved. As an example, since $\mathcal{Z}$ is proportional to either the canonical or microcanonical partition function (depending on the projection performed) and involves integration of a smooth integrand, it provides an alternative method for calculation of canonical correction factors which avoids the issue plaguing more standard approaches of highly oscillatory integrands. This is the subject of current work [23].

REFERENCES

1. *Fermi E.* // Prog. Theor. Phys. 1950. V. 5. P. 570.
2. *Hagedorn R.* // Nucl. Phys. B. 1970. V. 24. P. 93.
3. *Cleymans J. et al.* Thermal Model Analysis of Particle Ratios at GSI Ni–Ni Experiments Using Exact Strangeness Conservation // Phys. Rev. C. 1998. V. 57. P. 3319;
   Cleymans J., Oeschler H., Redlich K. Influence of Impact Parameter on Thermal Description of Relativistic Heavy Ion Collisions at GSI/SIS // Phys. Rev. C. 1999. V. 59. P. 1663;
   Averbeck R. et al. Neutral Pions and Eta Mesons as Probes of the Hadronic Fireball in Nucleus–Nucleus Collisions around $1A$ GeV // Phys. Rev. C. 2003. V. 67. P. 024903.
4. *Braun-Munzinger P. et al.* Thermal Equilibration and Expansion in Nucleus–Nucleus Collisions at the AGS // Phys. Lett. B. 1995. V. 344. P. 43.
5. *Braun-Munzinger P. et al.* Thermal and Hadrochemical Equilibration in Nucleus–Nucleus Collisions at the SPS // Phys. Lett. B. 1996. V. 365. P. 1;
   Braun-Munzinger P., Heppe I., Stachel J. Chemical Equilibration in Pb + Pb Collisions at the SPS // Phys. Lett. B. 1999. V. 465. P. 15;
   Becattini F. et al. Chemical Equilibrium in Nucleus–Nucleus Collisions at Relativistic Energies // Phys. Rev. C. 2004. V. 69. P. 024905.
6. *Adams J. et al.* (*STAR Collab.*). Experimental and Theoretical Challenges in the Search for the Quark–Gluon Plasma: The STAR Collaboration's Critical Assessment of the Evidence from RHIC Collisions // Nucl. Phys. A. 2005. V. 757. P. 102.

7. *Cleymans J. et al.* Comparison of Chemical Freeze-Out Criteria in Heavy-Ion Collisions // Phys. Rev. C. 2006. V. 73. P. 034905;
Cleymans J., Redlich K. Unified Description of Freeze-Out Parameters in Relativistic Heavy-Ion Collisions // Phys. Rev. Lett. 1998. V. 81. P. 5284–5286;
Becattini F., Manninen J., Gaździcki M. Energy and System Size Dependence of Chemical Freeze-Out in Relativistic Nuclear Collisions // Phys. Rev. C. 2006. V. 73. P. 044905;
Andronic A., Braun-Munzinger P., Stachel J. Hadron Production in Central Nucleus–Nucleus Collisions at Chemical Freeze-Out // Nucl. Phys. A. 2006. V. 772. P. 167.
8. *Kraus I. et al.* Statistical Model Predictions for $p-p$ and Pb–Pb Collisions at LHC. arXiv:0707.1282 [hep-ph];
Andronic A., Braun-Munzinger P., Stachel J. Thermal Model Predictions of Hadron Ratios at LHC. arXiv:0707.4076 [nucl-th];
Rafelski J., Letessier J. Strangeness Enhancement at LHC // J. Phys. G. 2008. V. 35. P. 044042;
Becattini F., Manninen J. Strangeness Production from SPS to LHC // J. Phys. G. 2008. V. 35. P. 104013.
9. *Andronic A. et al.* Statistical Hadronization of Charm: From FAIR to the LHC // Ibid. P. 104155.
10. *Wheaton S., Cleymans J., Hauer M.* THERMUS: A Thermal Model Package for ROOT // Comp. Phys. Commun. 2009. V. 180. P. 84.
11. *Karsch F., Laermann E., Schmidt C.* The Chiral Critical Point in Three-Flavor QCD // Phys. Lett. B. 2001. V. 520. P. 41;
Fodor Z., Katz S. D. Lattice Determination of the Critical Point of QCD at Finite T and μ // JHEP. 2002. V. 0203. P. 014;
Fodor Z., Katz S. D. Critical Point of QCD at Finite T and μ, Lattice Results for Physical Quark Masses // JHEP. 2004. V. 0404. P. 050.
12. *Hatta Y., Ikeda T.* Universality, the QCD Critical / Tricritical Point and the Quark Number Susceptibility // Phys. Rev. D. 2003. V. 67. P. 014028;
de Forcrand P., Philipsen O. The QCD Phase Diagram for Three Degenerate Flavors and Small Baryon Density // Nucl. Phys. B. 2003. V. 673. P. 170;
Schaefer B. J., Wambach J. Susceptibilities near the QCD (Tri)Critical Point // Phys. Rev. D. 2007. V. 75. P. 085015;
Fukushima K. Phase Diagrams in the Three-Flavor Nambu–Jona-Lasinio Model with the Polyakov Loop // Phys. Rev. D. 2008. V. 77. P. 114028;
Bowman E. S., Kapusta J. I. Critical Points in the Linear Sigma Model with Quarks // Phys. Rev. C. 2009. V. 79. P. 015202.
13. *Gaździcki M., Gorenstein M. I., Mrowczynski S.* Fluctuations and Deconfinement Phase Transition in Nucleus–Nucleus Collisions // Phys. Lett. B. 2004. V. 585. P. 115;
Gorenstein M. I., Gaździcki M., Zozulya O. S. Fluctuations of Strangeness and Deconfinement Phase Transition in Nucleus–Nucleus Collisions // Phys. Lett. B. 2004. V. 585. P. 237.
14. *Mishustin I. N.* Nonequilibrium Phase Transition in Rapidly Expanding QCD Matter // Phys. Rev. Lett. 1999. V. 82. P. 4779; Phase Transitions in Exploding Matter // Nucl. Phys. A. 2001. V. 681. P. 56–63;
Heiselberg H., Jackson A. D. Anomalous Multiplicity Fluctuations from Phase Transitions in Heavy-Ion Collisions // Phys. Rev. C. 2001. V. 63. P. 064904.
15. *Stephanov M. A., Rajagopal K., Shuryak E. V.* Signatures of the Tricritical Point in QCD // Phys. Rev. Lett. 1998. V. 81. P. 4816; Event-by-Event Fluctuations in Heavy Ion Collisions and the QCD Critical Point // Phys. Rev. D. 1999. V. 60. P. 114028;
Stephanov M. A. The Phase Diagram of QCD and the Critical Point // Acta Phys. Polon. B. 2004. V. 35. P. 2939;QCD Phase Diagram and the Critical Point // Prog. Theor. Phys. Suppl. 2004. V. 153. P. 139.

16. *Jeon S., Koch V.* Event-by-Event Fluctuations. arXiv:hep-ph/0304012;
Koch V. Hadronic Fluctuations and Correlations. arXiv:0810.2520 [nucl-th].
17. *Cheng M. et al.* Baryon Number, Strangeness and Electric Charge Fluctuations in QCD at High Temperature // Phys. Rev. D. 2009. V. 79. P. 074505.
18. *Hauer M., Torrieri G., Wheaton S.* Multiplicity Fluctuations and Correlations in Limited Momentum Space Bins in Relativistic Gases // Phys. Rev. C. 2009. V. 80. P. 014907.
19. *Hauer M., Wheaton S.* Statistical Ensembles with Finite Bath: A Description for an Event Generator // Ibid. P. 054915.
20. *Hauer M., Begun V. V., Gorenstein M. I.* Multiplicity Distributions in Canonical and Microcanonical Statistical Ensembles // Eur. Phys. J. C. 2008. V. 58. P. 83.
21. *Hauer M.* Multiplicity Fluctuations in Limited Segments of Momentum Space in Statistical Models // Phys. Rev. C. 2008. V. 77. P. 034909.
22. *Gorenstein M. I., Hauer M.* Statistical Ensembles with Fluctuating Extensive Quantities // Ibid. V. 78. P. 041902.
23. *de Klerk D., Hauer M., Wheaton S.* In preparation.